RESEARCH & DEVELOPMENT IN POWER ENGINEERING, 2019

Speciation of inorganic gaseous species and condensed phases during coconut husk combustion based on thermodynamic equilibrium calculations

Wojciech Jerzak[1,*], and *Monika* Kuźnia[2]

[1] AGH University of Science and Technology, Mickiewicza 30 Av., 30-059 Krakow, wjerzak@agh.edu.pl, Poland
[2] AGH University of Science and Technology, Mickiewicza 30 Av., 30-059 Krakow, kuznia@agh.edu.pl, Poland

Abstract. Thermodynamic equilibrium calculations to predict coconut husks (CH) combustion products have been carried out in this work. The selected type of biomass belongs to problematic fuels due to the fibrous structure preventing its grinding, and high chlorine content. The calculations results showed, that the combustion temperature for the tested range of 600-1000ºC clearly affects the concentrations of chlorine species in the flue gas. When the temperature was below 820°C, the highest concentration had HCl(g), and above 820°C KCl(g). The chlorine was also present in ash, as KCl-NaCl-RbCl solid solution, when the combustion temperature T ≤ 700°C, and KCl-NaCl-K_2SO_4-Na_2SO_4 liquid solution, when 600 ≤ T ≤ 960 °C. High content of chlorine in ash from CH combustion at T = 650°C has been confirmed experimentally. Speciations of inorganic gaseous species and condensed phases we investigated also during flue gas cooling from 1000 to 400ºC. Major condensed phase composition were dominated by alkali metal salts in both solid and liquid phase states. Finally, we presented sixteen eutectic points for different binary systems calculated in the FactSage software.

1 Introduction

The long-term European Union policy related to the reduction of CO_2 emissions from the fossil fuels combustion is an incentive for the development of technologies that use waste biomass for energy production. Biomass is considered as a renewable carbon-neutral fuel. However, there are many problems associated with the use of lignocellulosic biomass as a fuel, e.g.: high moisture content, low heating value, high chlorine, sulfur and alkali metal elements contents responsible for fouling, corrosion and slagging, and its fibrous structure makes biomass difficult to grind. The behaviour of the inorganic part of biomass during the combustion process [1-3], and cooling of products gas [4-7], can be determined by thermodynamic equilibrium prediction. The trends of the main solid and liquid phases formation as a function of combustion temperature under equilibrium conditions were investigated by Kaknics et al. [1]. They confirmed, among others that the low temperature of biomass combustion (below 800 °C) favors the formation of the alkali salts: KCl(s), NaCl(s), K_2SO_4(s), Na_2SO_4(s) in ash. Part of the potassium reacts with the biomass-ash in the combustion chamber forming silicates: $K_2Si_4O_6$(s), $Ca_3K_2Si_6O_{16}$(s) or $K_2Si_3MgO_8$(s). In turn, Wei et al. [2] indicated: KCl(g), KOH(g) and K_2SO_4(g) as the main constituents of the flue gas containing alkali. Furthermore, the air excess coefficient has a limited effect on the release of chlorine, potassium and sodium, whereas the increase in pressure can enhances the release of HCl(g) and reduces the formation of KCl(g), NaCl(g), KOH(g) and NaOH(g) at high temperatures. The release of inorganic gaseous species is controlled by the trace elements that compete for chlorine and sulfur [3]. Increased concentration of HCl(g) in the combustion chamber reduces the retention of Cd, Cu, Mn, Zn, Cr and Ni in the biomass-ash. During the cooling of the flue gas, the condensation of alkali salts vapors occurs. The vapors condensed, and can easily form the eutectics e.g. NaCl-KCl, NaCl-Na_2SO_4, with lower melting point than the pure salts [4, 5]. As reported by Froment et al. [6] condensation of K and Cl is favoured, when the total pressure is increased. The condensed phase formed when the gas is cooled contains not only salts, but also metal oxides and hydroxides such as: FeO(s), Fe_2O_3(s), Na_2O(s), NaOH(s,l) an KOH(s,l) [7].

2 Materials and Methods

2.1 Coconut husk

This work focuses on the fate of inorganics during coconut husk (CH) combustion. CH is an agricultural waste from coconut processing. The world leaders in coconut production are: Indonesia, Philippines, India, and Brazil [8]. CH is a high-calorie energy source containing a lot of lignin and cellulose. It has a large potential for use in power plants, due to availability and low price. At present, CH is used as domestic fuel, a fiber source for ropes, for biochar production, and as potential silica source [9, 10]. Table 1 presents proximate, ultimate and trace elements analysis of CH. All analyses were performed with three replicates in the Central Laboratory of Energopomiar in Gliwice, and Table 1 shows the mean

values. CH were tested in accordance with PN-EN ISO standards: 18134-2:2017-03 — Moisture, 18122:2016-01 — Ash, 18123:2016-01 — Volatile matter, 16948:2015-07 — C, H, and N, 16994:2016-10 — S, and Cl, 18125:2017-07 — Lower Heating Value (LHV), 16968:2015:07 — Trace elements. Whereas Hg determination was carried out in accordance with EPA Method 7473: 2007. CH contain as much as 1.9% chlorine. The chlorine accumulated in the husk comes from the fertilization system including sodium chloride or potassium chloride [8]. According to CH analysis, the molar ratio 2S/(K + Na) is 0.08. Values below 5 indicate a high propensity to create a deposit consisting of alkali chlorides [11]. In this case, the sulphation process reducing the tackiness of the deposit is very limited. There are also TEs present in CH among others: Rb, Sn, Pb, B, with concentrations above 10 mg/kg of dry fuel.

Table 1. Coconut husk analysis.

Proximate analysis (as received)	**%**
Moisture	8.5
Ash	5.39
Volatile matter	61.5
Calorific Value (dry)	**MJ/kg**
HHV	19.31
LHV	18.22
Ultimate analysis (dry)	**%**
C	49.59
H	5.3
N	0.38
S	0.06
Cl	1.9
O^{diff}	36.87
Trace elements (dry)	**mg/kg**
Zn	7.46
Cu	4.24
Pb	17.1
Ni	1.04
Cr	1.14
Cd	<0.06
Co	<0.1
As	<1
V	<0.5
Sb	<1.5
Ba	9.24
Sr	8.19
Mo	<3.2
Sn	17.8
Rb	47.1
Li	<0.15
B	11.8
Hg	0.008

TEs may react with chlorine and sulfur during combustion, so their identification in biomass plays an important role. As many as eighteen TEs listed in Table 1 were identified in CH, and Cd, Co, As, V, Sb, Mo, and Li were below the measurement range of the apparatus.

2.2 Ash

Ash from CH was obtained by biomass combustion at 650°C in an electric heated tube furnace. Chemical composition of ash included in Table 2 presents the average values from the three samples, and has been determined with the method of inductively coupled plasma optical emission spectrometry (ICP−OES) with the use of a plasma spectrometer Thermo iCAP 6500 Duo ICP. Chlorine and carbonates were determined according to the following standards: PN-EN 196-2: 2013-11, and PN-EN 15936: 2013-02. As can be seen from Table 2, silicon and potassium oxides predominate in the ash composition. Chlorine contained in ash accounts for 10.8 % of mass ash, which is in line with the value obtained by other researchers [12].

Table 2. Ash composition from CH at 650 °C

Component	**%**
SiO_2	31.6
Fe_2O_3	11.9
Al_2O_3	3.0
Mn_3O_4	0.10
TiO_2	0.30
CaO	2.33
MgO	2.19
P_2O_5	1.60
SO_3	1.12
Na_2O	4.82
K_2O	27.5
CO_2	1.5
Cl	10.8

2.3 Software and thermochemical database

Thermodynamic equilibrium calculations were performed in the Equilib module of the FactSage 6.3 commercial software. Thermodynamic equilibrium predictions are based on the minimizing of the total Gibbs free energy:

$$G = \sum_{\substack{ideal\\gas}} n_i \left(g_i^{\circ} + RT \ln p_i\right) + \sum_{\substack{pure\\condensed\\phases}} n_i \, g_i^{\circ} + \sum_{solution\ 1} n_i \left(g_i^{\circ} + RT \ln X_i + RT \ln \gamma_i\right) + \sum_{solution\ 2} n_i \left(g_i^{\circ} + RT \ln X_i + RT \ln \gamma_i\right) + \cdots \quad (1)$$

where:

$n_i, g_i^{\circ}, X_i, \gamma_i$ – successively moles, standard molar Gibbs energy, mole fraction, and activity coefficient of component "i",

p_i – partial pressure of the gas component "i",

R – universal gas constant,

T – temperature.

The system achieves thermodynamic equilibrium state, when:

$$G = min., \quad \text{or} \tag{2}$$

$$dG = 0 \tag{3}$$

The equilibrium criterion in equation (2) is mainly valid in multi-phase multicomponent systems.
In Equilib module, the following thermochemical databases were selected for pure components and solutions: FactPS, FToxide, ASalt-liq, FTpulp, and FTsalt. In addition, the Phase Diagram module was used to determine eutectic points in binary systems.

2.4 Calculation procedure

The calculation procedure covers two cases. The first is the combustion of 1 kg dry biomass, in the temperature range from 600 to 1 000 °C with a 20 °C steps, and λ=1.2. In the second case, the flue gas are cooled from 1 000 to 400°C, also with a 20°C step.

3 Result and discussion

3.1 Speciation of minor inorganic gaseous species calculated at different combustion temperature

The main flue gas components from CH combustion in the studied temperature range are: N_2>CO_2>H_2O>O_2>Ar. In addition, minor inorganic gaseous species are also present in the flue gas, the concentration of which varies with the combustion temperature. Figure 1 shows flue gas components present in minor quantities, i.e. ≥1 mg/m^3 wet flue gas. The fuel-bond chlorine during CH combustion reacts with potassium, hydrogen, sodium, and rubidium. When the combustion temperature is in the range of 600-780 °C, the flue gas are dominated by HCl. Increased concentration of HCl in the combustion chamber reduces the retention of Cd, Cu, Mn, Zn, Cr and Ni in the biomass-ash [3]. HCl have an inhibiting effect on biomass burning and CO → CO_2 oxidation [13]. HCl can easily be removed from the flue gas by a scrubbing process [13], or using an alkaline-carbonate sorbent [14], therefore, it belongs to the desired products containing chlorine. The following chlorides are also present in the flue gas: KCl, NaCl, RbCl, as dimers K_2Cl_2 and Na_2Cl_2. An increase in the combustion temperature above 780 °C, clearly promotes release of KCl, K_2Cl_2, NaCl, and reduction of HCl. As a result, the KCl concentration is fivefold as high as HCl at 1000 °C. Due to its high propensity to form aerosols in the cooling process, KCl is an undesirable constituent of flue gas, that contributes to deposition and corrosion. Apart from NO, Na_2Cl_2 and SO_2 in flue gas two trace elements (Rb, and B) can also be observed as RbCl, H_3BO_3 and KBO_2. The positive correlation of the increase in the volume of flue gases with temperature (resulting from the decrease in density) is the reason for the reduction of RbCl concentration in Fig. 1.

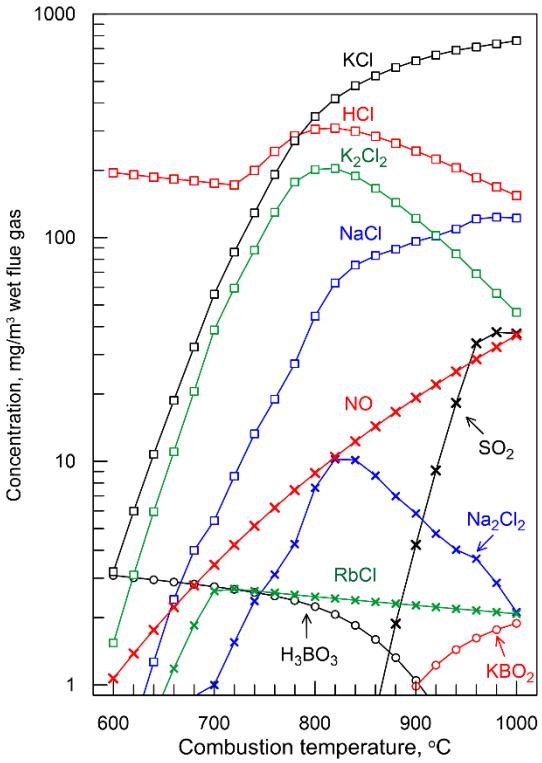

Fig. 1. Speciation of minor inorganic gaseous species (≥1 mg/m^3) during CH combustion in air.

3.2 Speciation of the condensed phase during CH combustion

The condensed phases shown in Fig. 2 are divided into three groups: a) alkali metal salts (solid and liquid), b) other solid salts, and c) solid oxides. Caring for the readability of Fig. 2, ash components with concentrations below 0.1 g/kg ash, i.e. $BaCrO_4$ and $NiTiO_3$, were not included. Although the low combustion temperature (<700 °C) inhibits potassium and sodium evaporation, however, these alkali are susceptible to forming the liquid solution KCl-NaCl-K_2SO_4-Na_2SO_4 already at a temperature of 600 °C. As known, chlorides and sulphates present in the ash, they interact with each other, and the melting temperature of the mixture is lower than the melting temperature of the individual salts [15]. The maximum total mass of the liquid salt solution was achieved at 720 °C, and the disappearance of the liquid phase at 980 °C. Potassium, sodium and rubidium chlorides in their solid state are formed only in the temperature range of 600 – 700 °C. According to Fig. 2b), the masses of individual solid ash components are conditioned by the combustion temperature. Only three solid salt compounds are present in the ash in the entire temperature range tested, ie. KAl_2SiO_6, $Na_2Ca_3Si_6O_{16}$, and $SrTiO_3$. Other salts are contained in the ash only in specific temperature ranges, with noticeable

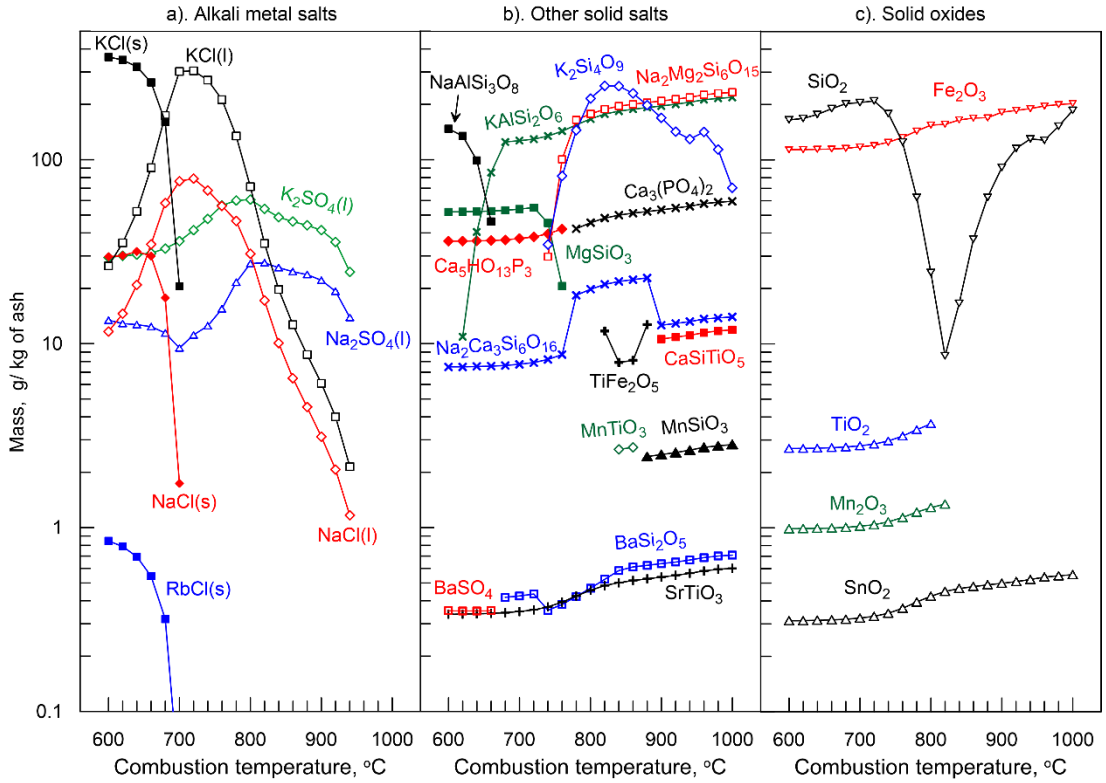

Fig. 2. Speciation of the condensed phase during CH combustion: a). alkali metal salts, b). other solid salts, and c). solid oxides.

transformations, e.g. $Ca_5HO_{13}P_3$ (T ≤ 860 °C) → $Ca_3(PO_4)_2$ (T ≥ 880 °C). In addition to salt, solid oxides are also thermodynamic predicted in ash: SiO_2, Fe_2O_3, TiO_2, Mn_2O_3, and SnO_2. The minimum SiO_2 concentration in Fig. 2c) occurs at the same temperature (820 °C) as the maximum $K_2Si_4O_9$ in Fig. 2b). The formation of potassium silicates depends on the molar ratios between the reactants and the gas atmosphere. When SiO_2:K_2CO_3 or SiO_2:KCl molar ratios is 4 or more, the formation of $K_2Si_4O_9$ occurs according to the reactions [16,17]:

$$4SiO_{2(s)} + K_2CO_{3(s)} \rightleftharpoons K_2Si_4O_{9(g)} + CO_{2(g)} \quad (4)$$

$$4SiO_{2(s)} + KCl_{(l)} + H_2O_{(g)} \rightleftharpoons K_2Si_4O_{9(g)} + 2HCl_{(g)} \quad (5)$$

3.3 Speciation of the condensed phase during the flue gas cooling

Condensable components during the flue gas cooling, was shown in Figs. 3a-b). Major condensed phase composition is dominated by alkali metal salts in both solid and liquid phase states. The liquid KCl-NaCl-K_2SO_4-Na_2SO_4 salt solution begins to form after the flue gas has been cooled to 960 °C. The flue gas cooling promotes an increase in the mass of liquid salt solution up to a temperature of 700 °C. The equilibrium between alkali (Me = K, or Na) chlorides and sulphates is determined on the basis of a series of reactions in which reactions (6) and (7) plays a leading role [18]:

$$2MeCl_{(g)} + H_2O_{(g)} + SO_{2(g)} + \tfrac{1}{2}O_{2(g)} \rightleftharpoons Me_2SO_{4(l)} + 2HCl_{(g)} \quad (6)$$

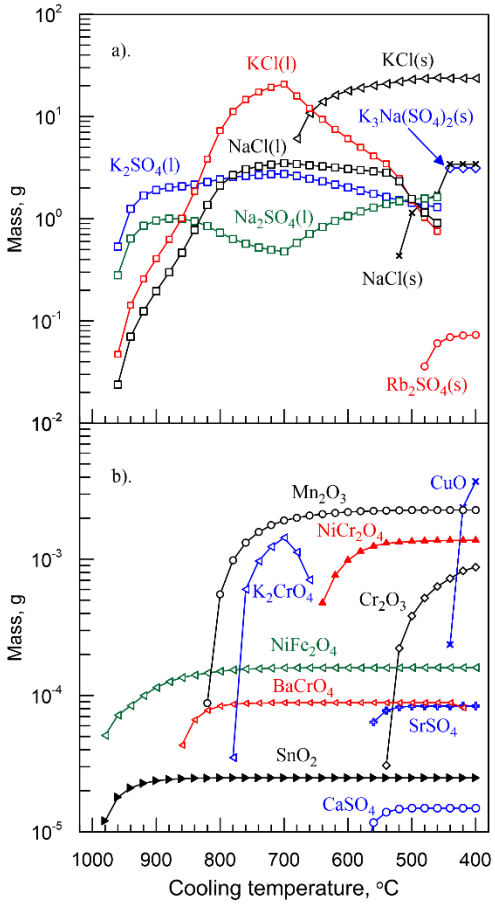

Fig. 3. Speciation of the condensed phase during the flue gas cooling: a). major condensed species, b). minor solid species.

$$2MeCl_{(g)} + SO_{2(g)} + O_{2(g)} \rightleftharpoons Me_2SO_{4(l)} + Cl_{2(g)} \quad (7)$$

As a result, the cooled flue gas contains less NaCl(g) and KCl(g), while more HCl(g) and $Cl_{2(g)}$. Further HCl(g) reacts with oxygen, according to the Deacon reaction:

$$2HCl_{(g)} + \tfrac{1}{2}O_{2(g)} \rightleftharpoons Cl_{2(g)} + H_2O_{(g)} \quad (8)$$

and the content of Cl_2 increases in the flue gas.
According to Fig. 3b), minor solid species (< 0.01g) are also forming in the flue gas cooling process. The cooler the flue gas, the more species it condenses (for example, at 980°C there are only two species, while at 420 °C as many as nine. Interestingly, based on thermodynamic prediction, condensed species form both salts and metal oxides. In the entire studied temperature range, only $NiFe_2O_4$ and SnO_2 have condensed. The remaining condensed components were only present in specific temperature ranges.

3.4 Eutectic points

In order to supplement the analysis of the occurrence of liquid species in the process of CH combustion and exhaust gas cooling, additional calculations were performed using the Phase Diagram module, determining eutectic points in binary systems. All calculations were carried out for a pressure of 1 atm, and the shares of components in binary systems were given in mass %. Calculations were made for sixteen binary systems, and the system with the lowest liquid temperature is presented in Fig. 4. The eutectic point for the $FeCl_2$–KCl phase diagram is determined by the composition of 48% mass KCl and 52% mass. $FeCl_2$ at 351°C.

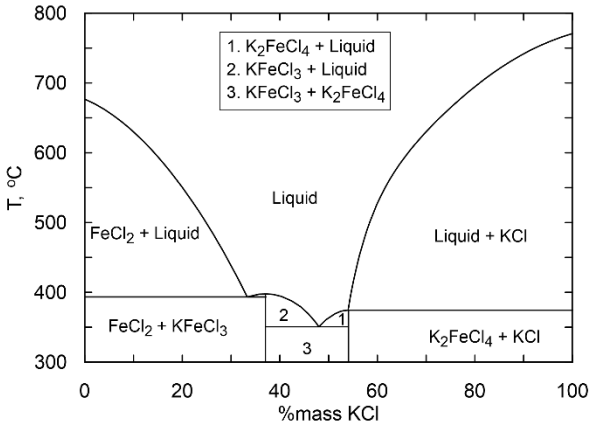

Fig. 4. Binary phase diagram of $FeCl_2$–KCl – calculated in the FactSage software.

The calculation results for selected binary systems are summarized in Table 3. The values are ordered according to lowest melting temperature, corresponding to the eutectic point. At this point, it should be emphasized that only binary phase systems are listed in Table 3, for which thermodynamic databases have already been developed. The authors of this article are aware of the need for further research in order to create databases for other systems, eg KCl-Na_2SO_4 (515 °C, 57% mass KCl) [19].

Table 3. Eutectic points for different binary systems calculated in the FactSage software.

System	Eutectic temperature, °C	Composition at eutectic point, mass %
KCl–$FeCl_2$	351	48
K_2CO_3–KOH	365	20
K_2SO_4–KOH	385	17
KCl–KOH	392	1→20
KCl–$PbCl_2$	408	20
K_2SO_4–Li_2SO_4	549	26
NaCl–RbCl	550	27.6
K_2O–SiO_2	584	61
KCl-$CaCl_2$	601	67
K_2O–Na_2O	602	84
KCl–K_2CO_3	617	47
NaCl-Na_2SO_4	625	32
KCl–NaCl	657	58.6
KCl–K_2SO_4	691	56
Na_2O –Na_2SO_4	781	11
K_2SO_4–Na_2SO_4	824	30

4 Conclusions

In this work, thermodynamic equilibrium calculations were performed in the FactSage 6.3 software, with the customized thermodynamic database for predicting the elemental composition of gaseous species and condensed phases under different temperature. Based on thermodynamic prediction, it has been shown that the dominant inorganic gaseous species of flue gas are: KCl(g), HCl(g), K_2Cl_2(g), and NaCl(g). Interpreting the calculation results of the combustion process, three groups were distinguished among condensed phases: a) alkali metal salts (solid and liquid), b) other solid salts, and c) solid oxides. KCl(s), NaCl(s) and RbCl(s) are formed only in the temperature range of 600 – 700 °C. It has been shown, that solid and liquid ash components are dependent by the combustion temperature. The consequence of flue gas cooling was the formation of a condensed phase. The phase composition was dominated by alkali metal salts in both solid and liquid states. The more strongly the exhaust gases were cooled, the more species of condensed phases therein were revealed. Finally, we analyzed sixteen binary systems for which eutectic points were determined.

This work was financially supported by the AGH University of Science and Technology (D.S. no. 16.16.110.663).

References

1. Kaknics J., Defoort F., Poirier J., *Energy Fuels*, Vol. 29, pp. 6433−6442, (2015).

2. Wei X., Schnell U., Hein K.R.G., *Fuel,* Vol. 84, pp. 841–848, (2005).
3. Miller B., Dugwell D.R., Kandiyoti R., *Energy Fuels,* Vol. 17, pp. 1382-1391, (2003).
4. Wang Y., Tan H., Wang X., Cao R., Wei B., *Fuel,* Vol. 187, pp. 33–42, (2017).
5. Lindberg D., Niemi J., Engblom M., Yrjas P., Laurén T., Hupa M., *Fuel Processing Technology*, Vol. 141, pp. 285–298, (2016).
6. Froment K., Defoort F., Bertrand C., Seiler J.M., Berjonneau J., Poirier J., *Fuel,* Vol. 107, pp. 269–281, (2013).
7. Wan W., Engvall K., Yang W., Fredriksson Möller B., *Energy*, Vol. 153, pp. 35–44, (2018).
8. Krishnakumar V., Thampan P.K., Achuthan Nair M., *The Coconut Palm (Cocos nucifera L.) - Research and Development Perspectives*, Springer Nature Singapore, (2019).
9. Suman S., Gautam S., *Energy Sources, Part A: Recovery, Utilization, and Environmental Effects,* Vol. 39(8), pp. 761–767, (2017).
10. Anuar M.F., Fen Y.W., Mohd Zaid M.H., Matori, K. A., Mohamed Khaidir R. E., *Results in Physics,* Vol. 11, pp. 1–4, (2018).
11. Robinson A.L., Junker H., Baxter L.L., Energy Fuels, Vol. 16, pp. 343-355, (2002).
12. Bonneau X., Haryanto I., Karsiwan T., Experimental Agriculture, Vol. 46 (3), pp. 401–414, (2010).
13. Glarborg P., *Computer Aided Chemical Engineering*, Vol. 45, pp. 603-645, (2019).
14. Ren X., Rokni E., Liu Y., Levendis Y.A., *Journal of Energy Engineering*, Vol. 144(4), 04018045, (2018).
15. Billen P., Van Caneghem J., Vandecasteele C., *Waste and Biomass Valorization*, Vol. 5, pp. 879–892, (2014).
16. Anicic B., Agglomeration Mechanisms during Fluidized Bed Combustion of Biomass. Kgs. Lyngby: Technical University of Denmark (DTU), (2018).
17. Defoort F., Dupont C., Durruty J., Guillaudeau J., Bedel L., Ravel S., Campargue M., Labalette F., Da Silva Perez D., Energy Fuels, Vol. 29, pp. 7242-7253, (2015).
18. Scandrett L.A., Clift R., *Journal of the Institute of Energy*, Vol. 57(433), pp. 391–397, (1984).
19. Rowe J.J., Morey G.W., Zen C.S., The Quinary Reciprocal Salt System Na, K, Mg, Ca/Cl, SO_4 – A Review of the Literature with New Data, Geological survey professional paper 741, US Govt. Print. Off., (1972).